Original Article

Incremental value of contrast enhanced computed tomography on diagnostic accuracy in evaluation of small pulmonary ground glass nodules

Ming Li[1*], Feng Gao[1*], Jayender Jagadeesan[2], Ritu R. Gill[2], Yanqing Hua[1], Xiangpeng Zheng[1]

[1]Department of Radiology and Radiation Oncology, Huadong Hospital affiliated to Fudan University, Shanghai, China; [2]Department of Radiology, Brigham and Women's Hospital affiliated to Harvard Medical School, Boston, Massachusetts, USA

*These authors contributed equally to this work.

Contributions: (I) Conception and design: M Li, F Gao, X Zheng; (II) Administrative support: Y Hua, X Zheng; (III) Provision of study materials or patients: M Li, F Gao; (IV) Collection and assembly of data: M Li, F Gao; (V) Data analysis and interpretation: M Li, J Jagadeesan, RR Gill, X Zheng; (VI) Manuscript writing: All authors; (VII) Final approval of manuscript: All authors.

Correspondence to: Xiangpeng Zheng. Department of Radiology and Radiation Oncology, Huadong Hospital affiliated to Fudan University, West 221 Yan'an Road, Shanghai 200040, China. Email: zhengxp@fudan.edu.cn.

Background: To evaluate the information gain by the application of both non-contrast and contrast enhanced computed tomography (CT) with extended mediastinal display window settings in the evaluation of pure ground glass nodules (pGGNs) and or mixed ground glass nodules (mGGNs) in the context of pre-invasive or early stage lung adenocarcinoma.

Methods: One hundred and fifty patients with ground glass nodules (GGNs) and mGGNs, with contrast enhanced CT scans within 2 weeks of thoracic surgery were included in the study. Quantitative evaluation of all nodules was performed in a conventional mediastinal window (CMW) and an extended mediastinal window (EMW) both on non-contrast images and contrast-enhanced images.

Results: Contrast-enhanced images with CMW demonstrated amplification of solid portion in 23 (43%), 41 (77%) with EMW out of 53 minimally invasive adenocarcinoma (MIA) nodules, and in 34 of 37 (91%) of invasive adenocarcinoma (IAC) nodules. Using the increase in size of solid portion of the nodule measured on the enhanced CT images with EMW, area under the receiver operating characteristic (ROC) curve of 0.872 and 0.899 was utilized for differentiating between the pre-invasive nodules and MIA and between MIA and IAC nodules, respectively. Statistically significant differences existed between the pre-invasive and the MIA groups, and MIA and the IAC groups in smaller nodules ($P<0.01$).

Conclusions: Comparative quantitative analysis of the pre and post contrast images can help differentiate between atypical adenomatous hyperplasia (AAH), adenocarcinoma in situ (AIS), MIAs, and IACs. Extension of the CT mediastinal window setting improves the evaluation of small GGNs, and can augment the diagnostic accuracy when evaluating small pGGNs and mGGNs.

Keywords: Lung adenocarcinoma; ground glass nodules (GGNs); window width/window level; tomography; X-ray computed; enhancement

Submitted Jun 20, 2015. Accepted for publication Sep 02, 2015.
doi: 10.3978/j.issn.2072-1439.2015.09.37
View this article at: http://dx.doi.org/10.3978/j.issn.2072-1439.2015.09.37

Introduction

Pulmonary ground glass nodules (GGNs) are defined as a nodular area of focal increase in density on a computed tomography (CT) scan precluding vessels and or airways. Based on the morphology, GGNs can be classified as pure ground glass nodules (pGGNs), or mixed ground glass nodules (mGGNs) (1). The recent Fleischner Society guidelines for follow up and management of part solid nodules allow for appropriate recommendations for GGN's, which can present as peripheral adenocarcinomas (2). However the uncertainty and inability to differentiate benign form malignant and pre-invasive and invasive adenocarcinomas (IACs) on qualitative assessment alone continues. Poor inter-observer and intra-observer agreement on accurate measurement of part solid lesions further adds to the interpretive variability, thus adversely affecting follow up and management of GGN's with greater potential for misclassification.

The new classification recommends that the terminology bronchioloalveolar carcinomas (BAC) be replaced in standard reporting by the terms adenocarcinoma in situ (AIS), minimally invasive adenocarcinoma (MIA), and IAC. Atypical adenomatous hyperplasia (AAH) and AIS are considered pre-invasive lesions (2-4). However all these lesions, AAH, AIS, MIA, and IAC can manifest as pGGN or mGGN with varying component of solid portion on CT images. Adding to the conundrum the volume doubling times of these lesions can vary up to 7 years and no clear plateau has been observed that could support termination of follow up of part solid lesions (4). Moreover, all the currently available CAD software has limited reliability and reproducibility when assessing part solid lesions (5). Qualitative radiographic assessment of GGN's can be affected by respiratory motion and indistinct borders with the adjacent lung parenchyma and can result in false positive and false negative assessments (5). Therefore more innovative methods are needed to improve the diagnostic accuracy of these lesions.

Many researchers have evaluated and confirmed the value of enhancement on CT scans in differentiating benign from malignant solid nodules (6,7). However, it is not known whether contrast enhancement receiver the differential diagnosis (DDx) of GGNs. Conventional mediastinal window (CMW; W/L =350/50 HU) are used in standard practice to evaluate the enhancement of solid nodules after contrast CT scan. We aimed to explore the value of using an extended mediastinal window (EMW; W/L =700/100 HU) setting in the evaluation of the enhancement and DDx of GGNs in comparison with the CMW setting. The purpose of this study was to evaluate the incremental utility of contrast enhancement in evaluation of ground glass and mGGNs in improving diagnostic accuracy.

Materials and methods

The institutional review board (IRB) of the Huadong Hospital, which is affiliated with Fudan University, approved this retrospective study. The requirement for patient informed consent was waived by the IRB.

Study population

One hundred and fifty patients with no prior history of malignancy including 46 men and 104 women with a mean age of 57.41±10.33 years (range, 30-78 years) were enrolled in this study between February 2011 and March 2014. Pre- and post-contrast CT scans were acquired within 2 weeks of surgical resection. These images were analysed and compared retrospectively with pathology as the gold standard. Inclusion criteria included GGN size of less than 2 cm along the largest dimension (lesion size was measured on thin-section images (1.25 mm). All nodules were classified as pGGNs, or mGGNs with solid portions of less than 5 mm in unenhanced CT images (lung window settings).

CT examination

Chest CT imaging (ranging from the apex to the base of the lung, including the chest wall and the axillary fossa) was performed on a 64-detector CT system (GE Light Speed VCT or GE Discovery CT750 HD, GE Healthcare, Milwaukee, WI, USA).The standard scan procedure for this type of patients in our hospital is to perform the non-contrast CT followed by contrast-enhanced CT. The following scan parameters were used are as follows—section width: 1.25 mm; reconstruction interval: 1.25 mm; pitch: 0.984; Tube voltage and current: 120 kV and 250 mA; display field of view (DFOV) ranged from 28 to 36 cm; matrix size: 512×512; pixel size ranged from 0.55 to 0.7 mm. All patients received a bolus of 80-100 mL of intravenous contrast medium [Optiray; Mallinckrodt Imaging, Hazelwood, MO, USA (350 mg iodine per mL)] at a rate of 3-4 mL/s using a power injector via an 18- or 20-gauge cannula in an antecubital vein. The enhanced CT scan commenced

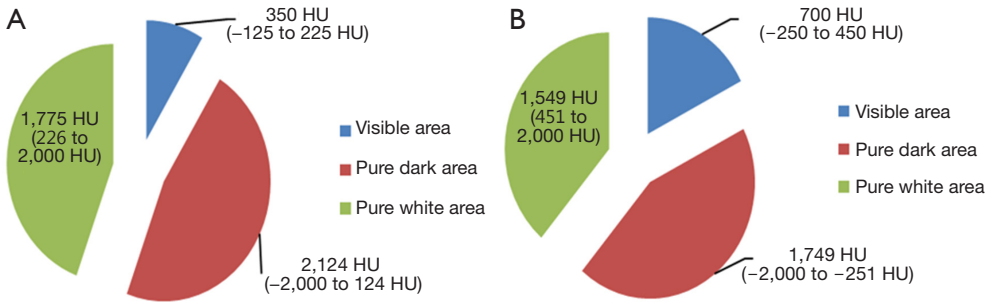

Figure 1 (A) CT values range (CMW); (B) CT values range (EMW). CMW, conventional mediastinal window; EMW, extended mediastinal window; CT, computed tomography.

60 seconds after the administration of the contrast medium (8). Both the standard and high-resolution reconstruction kernels were used for image reconstructions.

Pathological analysis

Based on the recommendations provided in the new classification system of lung adenocarcinomas, GGNs were resected by video-assisted thoracoscopic surgery. Specimens were fixed in 10% formalin and embedded in paraffin. Representative hematoxylin-eosin stained sections were reviewed. Cases that resulted in indistinct pathological classifications under light microscopy were confirmed by immune-histochemical analyses. All histological preparations and analyses were performed by two senior pathologists, according to the guidelines provided in the new classifications of lung adenocarcinomas (2). The diagnostic criteria were as follows: (I) AAH: local GGO lesions (usually less than 5 mm in diameter), mild or moderate atypical hyperplasia of the epithelial cells and lepidic growth along the alveolar wall without an inflammatory reaction of the mesenchyma or fibrous proliferation; (II) AIS: local lesions (no more than 3 cm), lepidic growth along the alveolar wall of tumorous cells without invasion of the vessels, pleura, or mesenchyma; (III) MIA: local lesions (no more than 3 cm) demonstrating predominantly lepidic growth and an extent of invasion of no more than 0.5 cm; (IV) IAC: local lesions (no more than 3 cm) with an extent of invasion greater than 0.5 cm.

CT imaging analysis

Two chest radiologists who were blinded to the pathology results evaluated the CT scans concurrently. The CT value measurement method of pGGNs was as follows: three regions of interest (ROIs) were measured, and the mean values on unenhanced and contrast-enhanced CT images were calculated. The ROI size was chosen to be 2×2 mm^2 for pure GGNs and 1×1 mm^2 form GGNs. ROIs were placed in the solid portions of mGGNs both in CMW and EMW (*Figure 1*). A quantitative evaluation of the largest dimensions of mGGNs was performed using a CMW and EMW, and the mean attenuations were computed in the ROI. When selecting an ROI, the vessels in both pGGNs and mGGNs were carefully excluded. For every GGN case, each radiologist independently reported the lesion location, GGN type, largest dimension of the solid portions of the mGGN, CT values of each pGGN on pre- and post-contrast-enhanced CT images, the likelihood of malignancy, and classified the nodule based on the new classifications of lung adenocarcinomas published in 2011 (1).

We evaluated nodule enhancement by analysing the non-contrast and contrast-enhanced CT images, and dividing the lesions into two categories. Category A was further subdivided into Category A1: no enhancement, and Category A2: elevation of mean CT value but absence of solid portions were found both in non-contrast and contrast enhanced CT images. The enhancement of these nodules was defined by measuring CT values of ROIs in non-contrast and contrast-enhanced CT images (*Figures 2,3*). Category B included enlargement of the solid portion of nodule after contrast, which could be subdivided into two types. In Category B1, no solid portions were observed on unenhanced CT images, but the solid portion was detected on contrast-enhanced CT images (*Figures 4,5*). In Category B2, solid portion (<5 mm) was noted on non-contrast CT images, as well as enlargement of the solid component size on the contrast-enhanced CT images (*Figure 6*). The largest dimension of the nodules was measured on the CMW setting (W/L =350/50 HU) and the EMW setting (W/L =700/100 HU), and the enhancement of nodules was evaluated by analysing the largest dimension of the solid portion both in CMW and EMW.

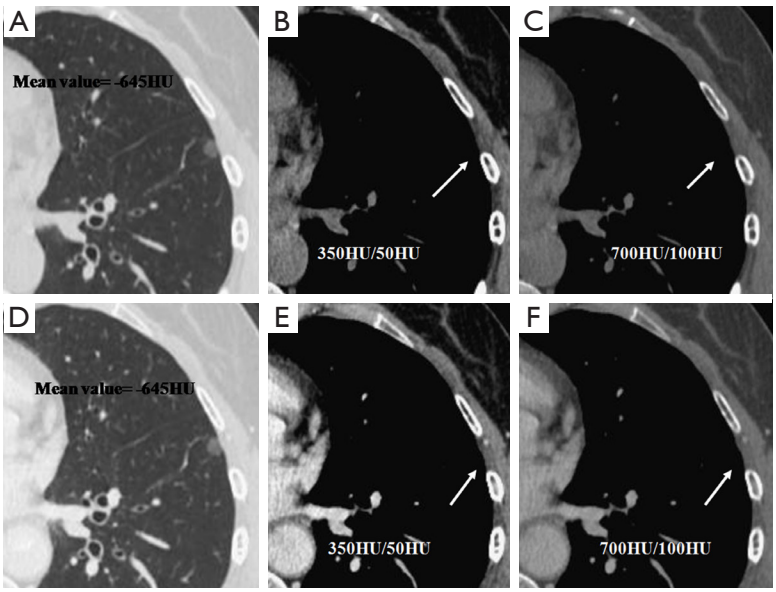

Figure 2 (A-F) A small pGGN (7 mm) in LLL, which was diagnosed as AAH by pathology. No solid portions were detected in plain and contrast CT images in CMW or EMW (arrows show the location of the nodule). No enhancement of this nodule was seen in CT. The mean CT values in (A) unenhanced CT image and (D) enhanced CT image were –645 HU. CT, computed tomography; pGGNs, pure ground glass nodules; CMW, conventional mediastinal window; AAH, atypical adenomatous hyperplasia; EMW, extended mediastinal window; LLL, left lower lobe.

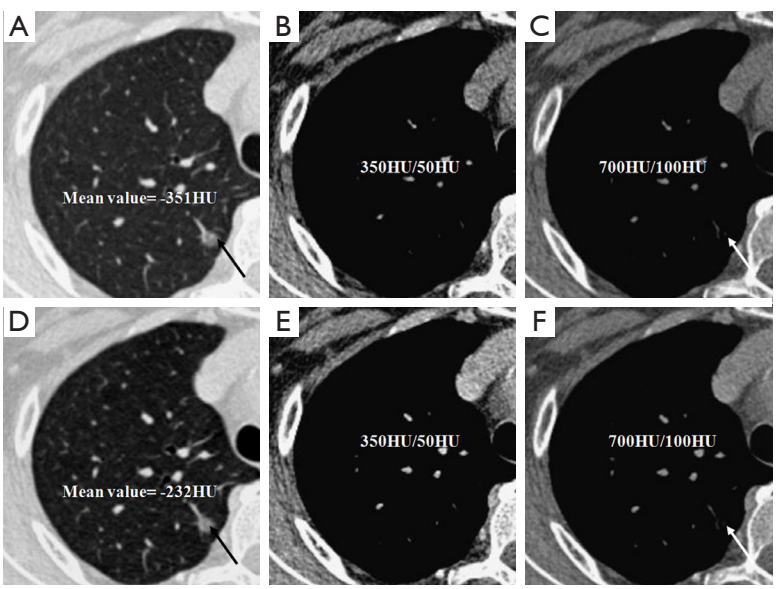

Figure 3 (A-F) A small pGGN diagnosed as AIS by pathology. No solid portions were detected in plain and contrast CT images in CMW and EMW (arrows in A, C, D, and F show the little vessel enhancement within the nodule that should not be considered as nodule enhancement). The enhancement of this nodule manifested as evaluation of mean CT values. The mean CT values in (A) unenhanced CT image and (D) enhanced CT image were –351 and –232 HU, respectively. CT, computed tomography; pGGNs, pure ground glass nodules; CMW, conventional mediastinal window; AIS, adenocarcinoma in situ; EMW, extended mediastinal window.

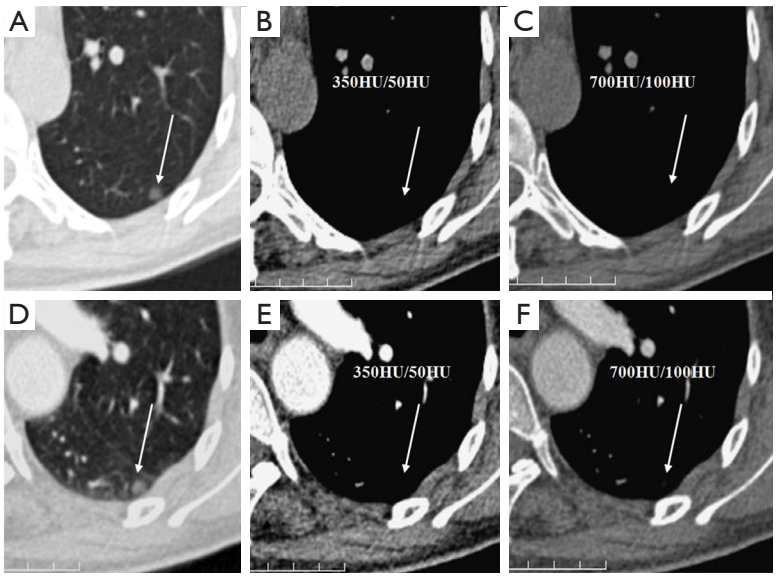

Figure 4 (A-F) A small pGGN (5 mm) in LLL. No solid portions were detected in plain and contrast CT images in CMW and EMW (arrows in A-F show the nodular enhancement indicated in F). The small GGN was diagnosed as AIS by pathology. CT, computed tomography; pGGNs, pure ground glass nodules; CMW, conventional mediastinal window; GGNs, ground glass nodules; AIS, adenocarcinoma in situ; EMW, extended mediastinal window; LLL, left lower lobe.

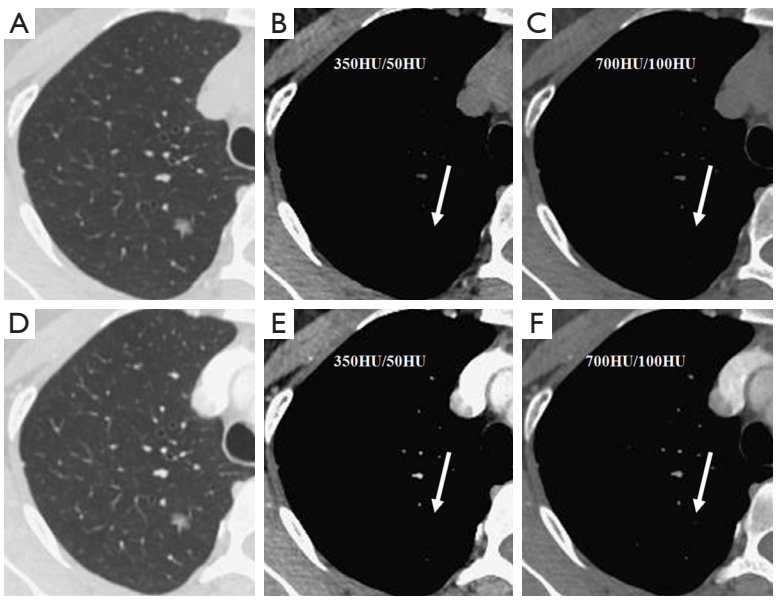

Figure 5 (A-F) A small pGGN (6 mm) with no solid portions in plain CT images in CMW and EMW, limited solid portions in EMW, and no solid portions in CMW (arrow in F shows enhancement of nodule beside the small vessel). This small pGGN was diagnosed as AIS by pathology. CT, computed tomography; pGGNs, pure ground glass nodules; CMW, conventional mediastinal window; AIS, adenocarcinoma in situ; EMW, extended mediastinal window.

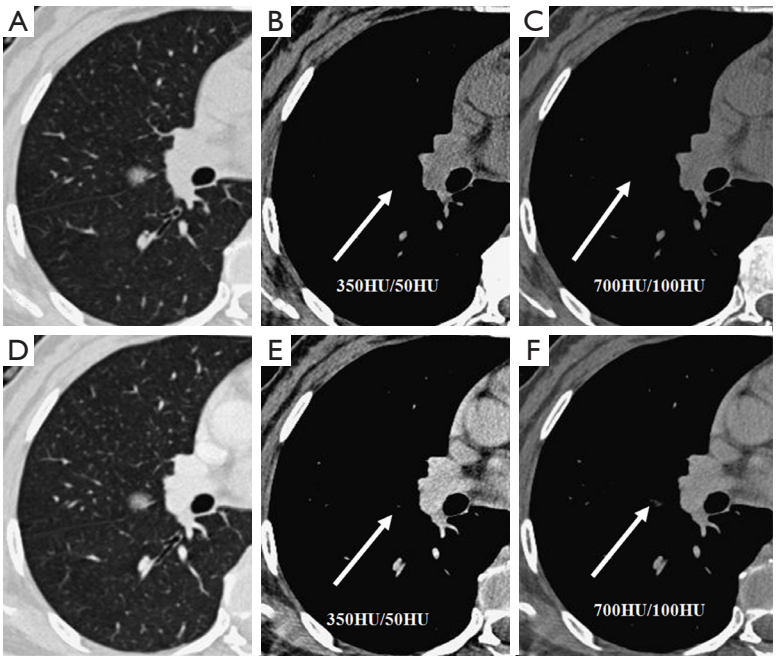

Figure 6 (A-F) A 9 mm mGGN (diagnosed MIA by pathology), with no solid portions in plain CT images, limited solid portions in EMW, and no solid portions in CMW (arrow in E shows the small vessel enhancement). The arrow in F shows the enhancement of the nodule beside the little vessel (EMW). CT, computed tomography; mGGNs, mixed ground glass nodules; CMW, conventional mediastinal window; MIA, minimally invasive adenocarcinoma; EMW, extended mediastinal window.

Statistical analysis

Statistical analyses were performed using a commercially available software program (SPSS 17.0 for Windows; SPSS, Chicago, IL, USA). The diagnoses of all nodules before surgery according to non-contrast and contrast-enhanced CT images of three different pathologic lesions were compared with the pathology diagnoses, and evaluated using Pearson's χ^2 test. Independent *t*-tests were used to compare age and GGN size among the different pathology groups (benign tumours, pre-invasive tumours, and IACs). Statistical results were considered significant when the P value was less than 0.05. A receiver operating characteristic (ROC) curve was calculated according to the largest dimensions of the solid portions of the nodules (both in CMW setting −350/50 HU and the EMW setting −700/100 HU) on both unenhanced and contrast-enhanced CT images, and the area under the curve (AUC) value was determined. For the analyses, AUCs between 0.50-0.70 were considered to have low diagnostic value, AUCs between 0.70-0.90 had medium diagnostic value, and AUCs above 0.90 had high diagnostic value.

Results

The 150 cases included 60 cases of pre-invasive lesions (8 AAH nodules and 52 AIS nodules), 53 MIA cases, and 37 IAC cases determined by pathology. In each group, there were more females than males. No statistically significant difference was observed between the pre-invasive and MIA groups, or the MIA and IAC groups for age (P=0.076 and P=0.470, respectively. However, statistically significant difference existed between the pre-invasive and MIA groups and the MIA and IAC groups with respect to nodule size (P=0.002 and P=0.001, respectively; *Table 1*).

Majority of pre-invasive nodules [56/60 (93%) in EMW and 59/60 (98%) in CMW respectively] manifested as increase in mean attenuation value on CT scan (mean value is 39.77 HU. Four nodules in the pre-invasive group using EMW manifested as enlargement of solid portion after contrast administration. In three of these four nodules with enlargement post contrast, no solid component was detected on the non-contrast CT images using the EMW. One of the four nodules had a 1 mm solid component on the non-contrast images and 2 mm solid component on contrast-

Table 1 Patient demographics

Items	Pre-invasive group	MIA group	IAC group
Gender			
Male	20	15	11
Female	40	38	26
Age (years)	55.63±11.13	59.21±9.94	57.70±9.28
Nodular size (mm)	6.89±2.32	8.57±3.13	10.99±3.17
Localization (nodules)			
RUL [60]	30	19	11
RML [9]	6	2	1
RLL [32]	8	11	13
LUL [33]	10	14	9
LLL [16]	6	7	3

IAC, invasive adenocarcinoma; MIA, minimally invasive adenocarcinoma; RUL, right upper lobe; RML, right middle lobe; RLL, right lower lobe; LUL, left upper lobe; LLL, left lower lobe.

Table 2 Enhancement manifestations of three groups

Comparison among groups	Elevation of mean CT values (HU)		Enlargement of solid portions in CMW (mm)		Enlargement of solid portions in EMW (mm)	
	Nodules	Mean ± SD	Nodules	Mean ± SD	Nodules	Mean ± SD
Pre-invasive	59 (CMW) 56 (EMW)	39.77±9.92	1	0.50±0.00	4	1.0±0.00
MIA	30 (CMW) 12 (EMW)	47.11±9.38	23	1.22±0.10	41	1.37±0.43
IAC	3 (CMW) 2 (EMW)	62.30±6.09	34	1.61±0.48	35	1.87±0.53
Pre-invasive *vs.* MIA	t=−4.03	P=0.000	t=−6.10	P=0.000	t=−10.39	P=0.000
MIA *vs.* IAC	t=9.31	P=0.000	t=8.50	P=0.000	t=4.865	P=0.000

CT, computed tomography; CMW, conventional mediastinal window; EMW, extended mediastinal window; IAC, invasive adenocarcinoma; MIA, minimally invasive adenocarcinoma.

enhanced CT. Increase in size of the solid portion was found in 23/53 MIA nodules (43%) on CMW settings and in 41/53 (77%) on EMW settings. Finally, the enlargement of solid component was detected in 34/37 (91%) of the IAC nodules on CMW and 35/37 (94%) in EMW settings. Statistically significant differences were observed between the pre-invasive and MIA groups, and MIA and IAC groups in terms of increase of mean CT Hounsfield values, as well as the enlargement of solid portions after contrast-enhancement in CMW and EMW (*Table 2*).

ROC analysis was performed and the areas under these curves were calculated in order to differentiate between pre-invasive, and MIA nodules, and MIA and IAC nodules with CMW and EMW in non-contrast and contrast-enhanced CT images (*Figures 4-8*) using the size of solid component within the nodule. The area under the ROC curve indicated that evaluation of the non-contrast CT images with CMW in order to differentiate between MIAs and pre-invasive nodules was of low value. Comparatively, higher diagnostic accuracy was observed for differentiating MIAs and IACs on the contrast-enhanced CT images with EMW (*Table 3*, *Figures 7*,*8*).

Pre-surgical diagnostic accuracy was no greater than 60% when measuring only solid portion of nodules on non-contrast CT images in the CMW setting and in the EMW setting. The differences between pathological and pre-surgical diagnoses according to non-contrast CT images were statistically significant (P<0.05). However, no statistically significant difference was found between the pathological and pre-surgical diagnoses when measuring solid portions of nodules on enhanced CT images captured in EMW (P>0.05; *Table 4*).

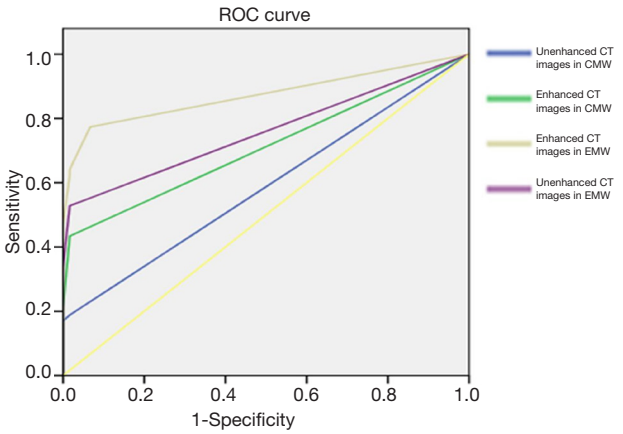

Figure 7 The resulting AUC following the differential diagnosis (DDx) of pre-invasive lesions and MIAs according to solid portions of nodules in plain and enhanced CT images in CMW setting at W/L =350/50 HU were 0.587±0.054 and 0.710±0.050, respectively. The resulting AUC in the EMW setting (W/L =700/100 HU) were 0.759±0.048 and 0.872±0.037, respectively. CT, computed tomography; CMW, conventional mediastinal window; MIA, minimally invasive adenocarcinoma; AUC, area under the curve; EMW, extended mediastinal window.

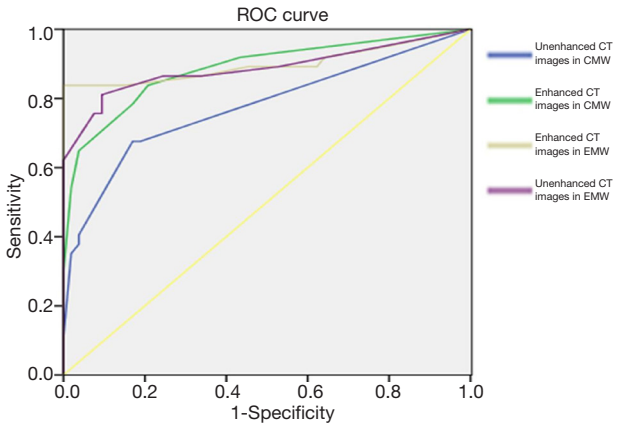

Figure 8 The resulting AUC following the differential diagnosis (DDx) of IACs and MIAs according to solid portions of nodules in plain and enhanced CT images in CMW setting at W/L =350/50 HU were 0.775±0.053 and 0.886±0.038, respectively. The resulting AUC in the EMW setting (W/L =700/100 HU) were 0.886±0.042, 0.899±0.042 respectively. CT, computed tomography; CMW, conventional mediastinal window; MIA, minimally invasive adenocarcinoma; IAC, invasive adenocarcinoma; AUC, area under the curve; EMW, extended mediastinal window.

Table 3 AUC values of ROC curves (DDx between pre-invasive nodules and MIAs, and MIAs and IACs according to solid portions of nodules measured in different window settings)

Items	DDx between pre-invasive nodules and MIAs	DDx between MIAs and IACs
Unenhanced images with CMW	0.587±0.054	0.775±0.053
Enhanced images with CMW	0.710±0.050	0.886±0.038
Unenhanced images with EMW	0.759±0.048	0.886±0.042
Enhanced images with EMW	0.872±0.037	0.899±0.042

DDx, differential diagnosis; CMW, conventional mediastinal window; EMW, extended mediastinal window; IAC, invasive adenocarcinoma; ROC, operating characteristic; AUC, area under the curve; MIA, minimally invasive adenocarcinoma.

Table 4 Pre-surgical diagnosis (according to measuring solid portions of nodules in unenhanced CT images and enhanced CT images) *vs*. pathological results

Items	Pre-invasive nodules	MIA	IAC	χ^2 value	P value*	Accuracy (%)
Unenhanced images with CMW	114	36	0	42.17	0.000	69 (46.00)
Enhanced images with CMW	92	58	0	31.64	0.000	82 (54.67)
Unenhanced images with EMW	88	62	0	30.11	0.000	87 (58.00)
Enhanced images with EMW	72	47	31	0.72	0.699	126 (84.00)
Pathological diagnosis	60	53	37			

*, values are obtained using the pathological results as the reference standard. CT, computed tomography; CMW, conventional mediastinal window; EMW, extended mediastinal window; IAC, invasive adenocarcinoma; MIA, minimally invasive adenocarcinoma.

Discussion

Our study evaluated and confirmed the incremental value of post contrast images and utility of extension of the CT mediastinal window settings in differentiating AAHs, AISs, MIAs, and IACs. The technique is simplistic in approach and can potentially be used in downstream pathways of nodule assessment when combined with Lung Cancer Screening. To the best of our knowledge, there has been no previous work that discusses the value of contrast-enhanced CT scan in differentiation of GGNs. It may be partially because the enhancement of GGNs is hard to define and quantify on the CMW settings. The GGN's are poorly represented on the CMW setting display, particularly when evaluating subtle contrast enhancement. Thus, we adjusted the window settings to improve visualization of enhancement in these lesions.

The CMW settings are 350/50 HU, and tissues with density ranging between −125 and 225 HU and can be best visualised on these settings, while the rest would either appear as pure black or pure white on these settings. Considering the CT Hounsfield value of most GGNs range between −400 to −750 HU (9,10), they are not visualized in these settings. Therefore the window settings need to be adjusted in the range that they can be visualized best. In order to allow for comparison with the CMW setting, we adjusted the window width/window level to 700/100 HU, to allow for display of images between −250 and 450 HU, in the EMW settings. In our study we observed the most significant incremental benefit of the EMW when evaluating MIA lesions. This can be crucial to patient management and can help with decision support in weather to longitudinally follow a nodule or resect it.

The pathophysiology of enhancement characteristics of nodule is based on angiogenesis within tumours (11,12). This is also true in GGNs, but since majority of these lesions do not have a solid component and the current practice to use non-contrast CT scans for evaluation, there is sparse if any literature on this subject. The solid component within of these nodules mostly represents fibrous proliferation, accumulations of multiple layers of tumour cells, surrounding invasion, the collapse of alveoli, and tumour cells, or secretions within the alveolar space. These can cause an increase in mean Hounsfield value on non-contrast CT images, and the degree of neo-vascularity in these lesions is further reflective of the degree of enhancement and can be indicative of the invasiveness of the tumour (13-17). Our data are consistent with this finding, the MIA and IAC lesions showed greater degree of enhancement as compared with AIS and the solid component which represents the invasive component measured larger post contrast.

Nakajima *et al*. (18) reported that 10% of pGGNs are IAC of lung. This phenomenon can be observed if the tumour has lepidic growth along the alveolar wall was in multiple layers, or if the lesions have acinar, papillary, micropapillary features. Even though these are all invasive features, but due to presence of air in the alveoli interspersed with the matrix, causes a pure GGN appearance on CT scans. Our study indicates that matched contrast enhanced CT scan thus improve diagnostic accuracy.

In our study, we observed that a high number of nodules manifested as enlargement of solid portions after contrast in EMW than CMW regardless of whether the lesion was categorised as pre-invasive, MIA, or IAC. Significant improvement in pre-surgical diagnosis was achieved in EMW but not in CMW. Further, no statistically significant differences in the diagnosis were detected between CT images (contrast-enhanced CT scan and observed in EMW) and pathology results ($P>0.05$). Thus, the amplification of the window width and window level of the CT mediastinal window setting could potentially increase the pre-surgical diagnostic accuracy of small and low-density nodules. There were some limitations of our research, such as the small sample size and inclusion of only malignant lesions. Inclusion of inflammatory lesions or other benign tumours may need to be considered in further refining management strategies, however these lesions are not generally resected and are longitudinally followed to clearance, therefore final pathological confirmation may not be possible.

Conclusions

In conclusion, comparative quantitative analysis of the pre and post contrast images in GGN and mGGN lesions can help differentiate between AAHs, AISs, MIAs, and IACs. Extension of the CT mediastinal window settings to EMW settings can further improve the evaluation of small GGNs, and can augment the diagnostic accuracy when evaluating small and part solid nodules. A prospective larger study with inclusion of benign lesions is needed in our follow up studies.

Acknowledgements

Funding: This work has been financially supported by the

National Natural Science Foundation of China (Grant No. 81472794), Shanghai Municipal Commission of Health (20134360), Shanghai Municipal Commission of Science and Technology (24119a0400), Key talents training program of Huadong Hospital (HDGG2014011).

Footnote

Conflicts of Interest: The authors have no conflicts of interest to declare.

References

1. Hansell DM, Bankier AA, MacMahon H, et al. Fleischner Society: glossary of terms for thoracic imaging. Radiology 2008;246:697-722.
2. Naidich DP, Bankier AA, MacMahon H, et al. Recommendations for the management of subsolid pulmonary nodules detected at CT: a statement from the Fleischner Society. Radiology 2013;266:304-17.
3. Travis WD, Brambilla E, Noguchi M, et al. International association for the study of lung cancer/american thoracic society/european respiratory society international multidisciplinary classification of lung adenocarcinoma. J Thorac Oncol 2011;6:244-85.
4. Hiramatsu M, Inagaki T, Inagaki T, et al. Pulmonary ground-glass opacity (GGO) lesions-large size and a history of lung cancer are risk factors for growth. J Thorac Oncol 2008;3:1245-50.
5. Chae HD, Park CM, Park SJ, et al. Computerized texture analysis of persistent part-solid ground-glass nodules: differentiation of preinvasive lesions from invasive pulmonary adenocarcinomas. Radiology 2014;273:285-93.
6. Yi CA, Lee KS, Kim EA, et al. Solitary pulmonary nodules: dynamic enhanced multi-detector row CT study and comparison with vascular endothelial growth factor and microvessel density. Radiology 2004;233:191-9.
7. Wang Y, Wang JA, Liang KR, et al. Correlations between tumor stroma characters and dynamic enhanced MDCT findings in nodular pulmonary adenocarcinoma. J Comput Assist Tomogr 2014;38:82-8.
8. Chae EJ, Song JW, Seo JB, et al. Clinical utility of dual-energy CT in the evaluation of solitary pulmonary nodules: initial experience. Radiology 2008;249:671-81.
9. Oda S, Awai K, Liu D, et al. Ground-glass opacities on thin-section helical CT: differentiation between bronchioloalveolar carcinoma and atypical adenomatous hyperplasia. AJR Am J Roentgenol 2008;190:1363-8.
10. Nomori H, Ohtsuka T, Naruke T, et al. Differentiating between atypical adenomatous hyperplasia and bronchioloalveolar carcinoma using the computed tomography number histogram. Ann Thorac Surg 2003;76:867-71.
11. Lee TY, Purdie TG, Stewart E. CT imaging of angiogenesis. Q J Nucl Med 2003;47:171-87.
12. Folkman J. Seminars in Medicine of the Beth Israel Hospital, Boston. Clinical applications of research on angiogenesis. N Engl J Med 1995;333:1757-63.
13. Yamashita K, Matsunobe S, Takahashi R, et al. Small peripheral lung carcinoma evaluated with incremental dynamic CT: radiologic-pathologic correlation. Radiology 1995;196:401-8.
14. Jain RK. Delivery of novel therapeutic agents in tumors: physiological barriers and strategies. J Natl Cancer Inst 1989;81:570-6.
15. Bettencourt MC, Bauer JJ, Sesterhenn IA, et al. CD34 immunohistochemical assessment of angiogenesis as a prognostic marker for prostate cancer recurrence after radical prostatectomy. J Urol 1998;160:459-65.
16. Weidner N. Intratumor microvessel density as a prognostic factor in cancer. Am J Pathol 1995;147:9-19.
17. Koukourakis MI, Giatromanolaki A, Thorpe PE, et al. Vascular endothelial growth factor/KDR activated microvessel density versus CD31 standard microvessel density in non-small cell lung cancer. Cancer Res 2000;60:3088-95.
18. Nakajima R, Yokose T, Kakinuma R, et al. Localized pure ground-glass opacity on high-resolution CT: histologic characteristics. J Comput Assist Tomogr 2002;26:323-9.

Cite this article as: Li M, Gao F, Jagadeesan J, Gill RR, Hua Y, Zheng X. Incremental value of contrast enhanced computed tomography on diagnostic accuracy in evaluation of small pulmonary ground glass nodules. J Thorac Dis 2015;7(9):1606-1615. doi: 10.3978/j.issn.2072-1439.2015.09.37

